XLIII CILAMCE
21–25, November, 2022
FOZ DO IGUAÇU – PR – BRAZIL

Numerical Modeling in Reinforced Concrete Tie Rods

Bruno Ricardo Ferreira de Oliveira[1], Eduardo de Moraes Rego Fairbairn[1], Rodolfo Giacomim Mendes de Andrade[2]

[1] *Civil Engineering Department of the Post-Graduate Institute of Federal University of Rio de Janeiro, COPPE/UFRJ, 149 Athos da Silveira Ramos Ave, 21941-909, Rio de Janeiro, Brazil.*
bruno.oliveira@coc.ufrj.br, eduardo.fairbairn@coc.ufrj.br
[2] *Civil Engineering Department of the Federal Institute of Espírito Santo, 1749 Vitória Ave, 29040-780, Vitória, Espírito Santo, Brazil.*
rodolfo.andrade@ifes.edu.br

Abstract. Concrete is a fragile material when subjected to tensile stresses, however, it is possible that a substantial contribution can be perceived in the design of reinforced concrete elements under tension, even in the post-cracking stage. In plain concrete, when the tensile strength is reached, cracks appear that progress until the material ruptures, this is a localized behavior known as “strain softening”. Different from plain concrete, reinforced concrete does not show softening due to the transfer mechanisms of tensile forces existing at the steel-concrete interface, so tensile stiffness is a phenomenon that occurs exclusively in reinforced concrete structures. The steel-concrete adhesion is directly related to energy absorption, which allows the redistribution of stresses between the materials after cracking, contributing to an increase in the strength and stiffness of the reinforced concrete element in an effect known as tension stiffening.

Keywords: Reinforced concrete, Tension stiffening, Finite elements, Reinforced concrete rods, Numerical modeling

1 Introduction

The use of the addition of steel bars to concrete for structural purposes has its relevance in the world scenario and the cracking behavior of reinforced concrete structures has been widely studied. The success of this result is largely due to the compatibility of tensions between these two materials and the absorption of the imposed energy, which is only possible due to a perfect adhesion between the concrete and the reinforcement. The concrete that originally has high compressive strength, has a brittle behavior under tensile stresses, even so, it can contribute to the strength of the part due to the effect called “tensile stiffening”. Tensile stiffening is the contribution to the stiffness of the bar of intact concrete between the primary cracks and plays a significant role in the deformation of reinforced concrete at service limit states, particularly in the case of lightly reinforced bars [8]. Tensile stiffness reflects the concrete's ability to support the stress between cracks, which increases the stiffness of a reinforced concrete element before the reinforcement yields [17]. The decline in tensile stiffening with increasing load is mainly attributed to the formation of new primary cracks during the crack formation phase due to adhesion degradation during the crack stabilization phase [8]. In this work, the results of numerical computational modeling of reinforced concrete rods by a three-dimensional analysis performed in the DIANA FEA software are analyzed and compared with experimental data of rods with single longitudinal reinforcement, in a specimen of dimensions 150x150x800 mm, for the concrete without mineral additions and fibers [17]. The use of computational numerical modeling is relevant and complements experimental studies to improve the understanding of different properties and parameters [1] ,[10].

2 Theoretical Conception

2.1 Tension Stiffness

Reinforced concrete elements submitted to uniaxial tension are subjected to an effect called tensile stiffening after cracking, in which the cracked concrete stiffness is less than the solid concrete stiffness [5].

The term "tensile stiffening" is defined as the effect of concrete acting in tension between cracks on the stress of steel reinforcement. In a crack, the internal tensile force is supported by the steel while between cracks, a part of the tensile force is transferred through bonding to the surrounding concrete, resulting in a reduction in the stresses and strains of the reinforcement and causes deformation. of the reinforcement in the non-cracked zone is smaller than the deformation of the reinforcement in the cracked region [4].

The tensile stiffening behavior can be generally characterized in a single reinforced concrete element in four phases as seen in Fig. 1, elastic phase (a), multiple crack phase (b), crack stabilization (c) and the steel yielding phase (d).

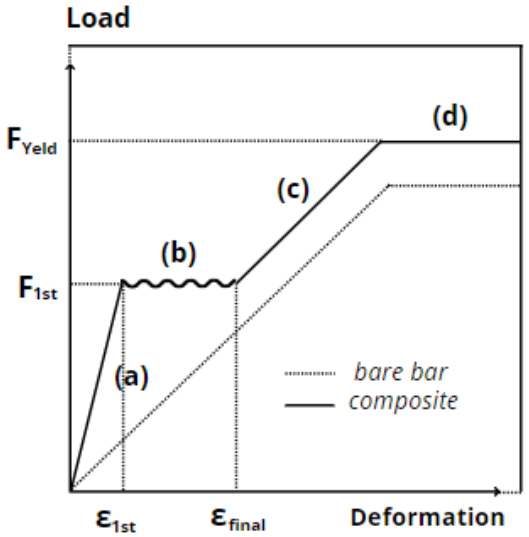

Figure 1. Typical behavior of the element in tensile test, adapted from [15].

In the elastic pre-cracking phase (section (a)), the load is distributed and the relative stiffness of the matrix and the reinforcement, under the assumption of perfect adhesion, distribute this load. The appearance of the first crack does not lead to a catastrophic failure, but it will result in a redistribution of load between the matrix and the bar. With the initiation of the first crack, the load is distributed, transferred to the steel and returned to the concrete through the adhesion properties. In the multiple crack phase (section (b)) it starts from the first crack load (F_{1st}) and the first crack deformation (ε_{1st}) and represents the tensile strength of the matrix. As cracking occurs in the brittle matrix, the load is transferred to the reinforcement, and further deformation will result in more cracks until the matrix is split into several segments. With the multi-crack phase, an approximately constant stress occurs, the matrix suffers a loss of strength and modulus of elasticity by the formation of each crack until it can no longer contribute substantially to the load carrying capacity. When there are no more multiple cracks and the concrete matrix is already divided by parallel cracks, any further deformation causes the reinforcement to detach and slip. Therefore, after the cracking phase, when the steel supports the tensile loads almost entirely, the composite still resists the increasing load (section (c)). In this phase the stiffness of the reinforcement supports the upward behavior of the load vs. axial deformation in the post-cracking zone. The composite curve in the post-crack zone also shows the curve of the isolated bar, as the behavior of the composite is governed almost entirely by the reinforcement at higher strain levels and it is possible to determine the post-crack equivalent modulus. The tensile load increases until the steel yield stage (line d) where the final yield load (Fyeld) can be obtained. Finally, failure occurs when the reinforcement reaches its maximum strength [2], [15] or the adhesion between the concrete and the reinforcement decreases [18].

3 Description of the FEM model

A geometric scheme was implemented, fully maintaining the geometry of the experimental model, the constraints and applied loads, as well as the constitutive laws of the materials are described below. The reinforced concrete rod was modeled with the DIANA FEA finite element software.

3.1 Geometric aspects

In order to compare the experimental results of Oliveira Júnior et al. [17], all geometric properties and boundary conditions were preserved. The tie rod has a square cross section of 150x150 mm and 800 mm in length, reinforced with a single steel bar, centered, as in Fig. 2.

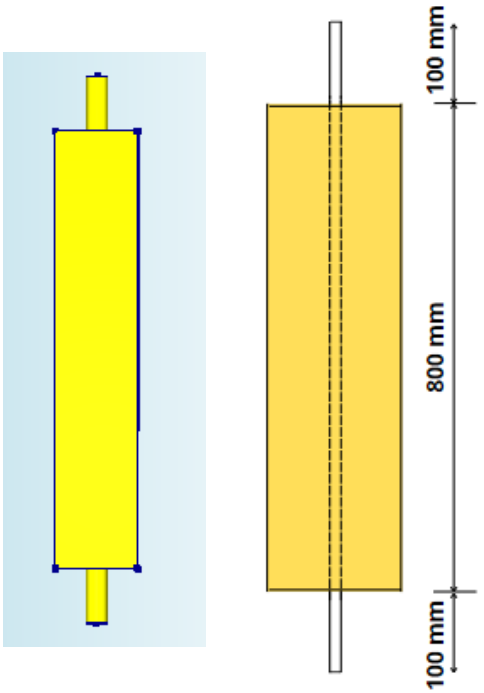

Figure 2. Geometric properties [17] (a) Diana FEA, (b) experimental.

The steel bar of the tie rod is 1000 mm long and 20 mm in diameter, it was positioned longitudinally to the axis of the specimen, leaving 100 mm of free steel at both ends to allow the application of a load, as described in Fig. 3 .

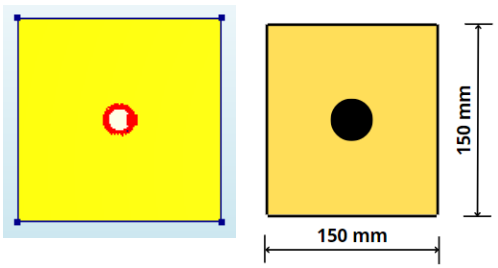

Figure 3. Geometric properties [17] (a) Diana FEA, (b)experimental.

3.2 Material properties in the experimental test

Oliveira Júnior et al. [17] produced the concrete by adding blast furnace slag, Portland cement, natural sand, coarse aggregate with a maximum size of 25 mm and superplasticizer additive (1%), the composition is shown in Tab. 1.

The reinforcement used was a single bar of CA-50 steel, with a diameter of 20 mm, has a yield point of 494 MPa and a modulus of elasticity of 210 GPa.

Material	Plain concrete
Cement	439.05
Natural sand	870.10
Coarse aggregate	870.10
Water	173.50
Superplasticizer	3.29
Workability (mm)	210

Table 1. Composition of concrete without mineral additions (kg m³).

The mechanical properties of plain concrete, without mineral additions, are given in Tab. 2.

Vf (%)	Plain concrete
fcm, Mpa	44,37
fctm, Mpa	4.20

Table 2. Mechanical properties of concretes without mineral additions.

3.3 Mesh properties

A three-dimensional mesh of solid elements was adopted for this study. The mesh is of the hexa quadratic type with elements measuring 20 mm (see Fig. 4.b) and adaptive sizes in the contact between bar x reinforcement (see Fig. 4.a). The finite element model of this study had a total of 3,646 elements in the bar and in the concrete body. For the concrete-reinforcement interaction, a perfect bond was adopted.

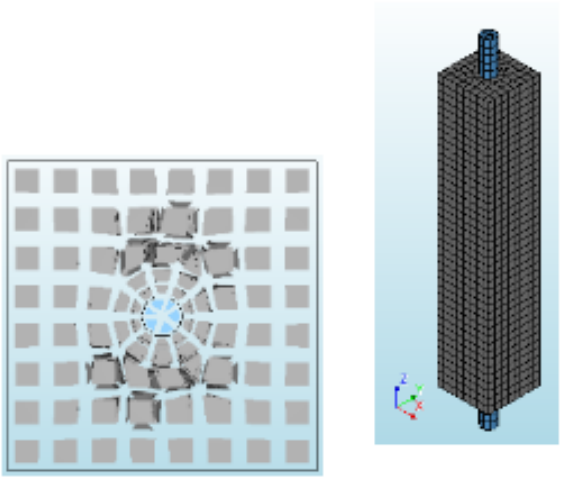

Figure 4. Top view adaptive mesh (a) isometric view of the composite (b) generated in DIANA FEA software.

The mesh featured regular solid finite elements of type CHX60, which is a twenty-node isoparametric solid element based on quadratic interpolation and Gaussian integration, CPY39, which is a thirteen-node isoparametric solid pyramid element based on quadratic interpolation and integration, CTP45 which is a fifteen-node isoparametric solid wedge element based on quadratic interpolation and numerical integration and finally the CTE30 element which is a ten-node, three-sided isoparametric solid tetrahedron based on quadratic interpolation and numerical integration [14].

3.4 Computational numerical modeling

A non-linear structural analysis was performed using the iterative method and the Newton-Raphson technique was used to solve the equations.

The computational test was piloted by a prescribed deformation of 3 mm in the longitudinal direction of the tie. To avoid rigid body displacement, restrictions were applied to the bar and the concrete, as can be seen in Fig. 5. At the base of the steel bar, movement restriction was applied in three directions (X,Y,Z) and at the top it was inserted support for the application of the prescribed deformation. In the concrete body the faces parallel to the X,Z axis were constrained only in the Y direction and the faces parallel to the Y,Z axis were constrained only in the X direction.

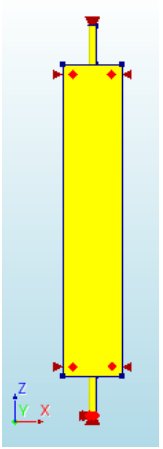

Figure 5. Supports of the computational model generated in the DIANA FEA software.

The input data to computationally represent the steel include, for the linear properties of the material, a modulus of elasticity of 210 GPa and a Poisson's ratio of 0.2 were used. For the plastic behavior, the Von Mises and Tresca plasticity model was adopted with a yield point of 492 MPa.

For concrete, a modulus of elasticity of 34.3 MPa, Poisson's ratio of 0.2 was adopted, for the constitutive law of traction, a study was carried out with different traction curves for analysis of compatibility with the experimental curve as observed in Fig. 6, having Hordijk's function was adopted with tensile strength of 4.2 MPa, fracture energy of 0.3 N/mm and for the compression law a parabolic curve with compressive strength of 44.37 MPa and fracture energy in compression of 35.97 N/mm.

4 Results and discussions

The diagrams were obtained by measuring the deformations of the reinforcement and the specimen. The load value shown on the ordinate axis is the result of the sum of all support reactions at each surface node where the prescribed deformation was applied at each load step (see Fig. 6).

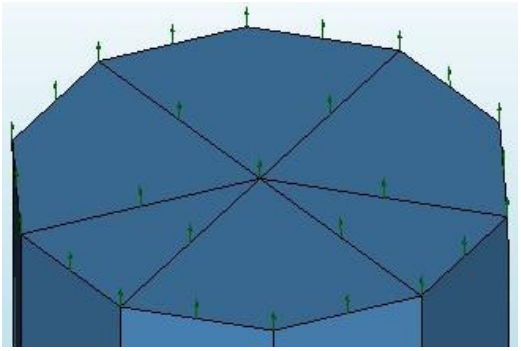

Figure 6. Nodes on the load application face generated in DIANA FEA software.

To obtain the deformations (ε) presented on the abscissa axis, two nodes were selected at the ends of the concrete body. For each applied load step, it is possible to measure the changes in the height of the element through the selected nodes and determine the value of the elongation ($\boldsymbol{\delta} = L - L_0$), where L is the distance between node A and node B and L_0 is the initial length of the element. concrete element, as can be seen in Fig. 7. Finally, the strains (ε) are calculated by dividing the elongation ($\boldsymbol{\delta}$) by the initial length (L_0).

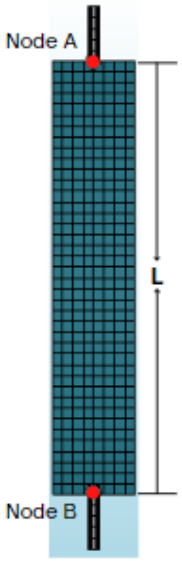

Figure 7. Determination of the elongation (**δ**).

To calibrate the numerical models, a comparative study of the curve model within the concrete tensile law was performed. The approximation results of the numerical and experimental curves are available in Fig. 8. The experimental curve of the direct tension test of the bar is also presented.

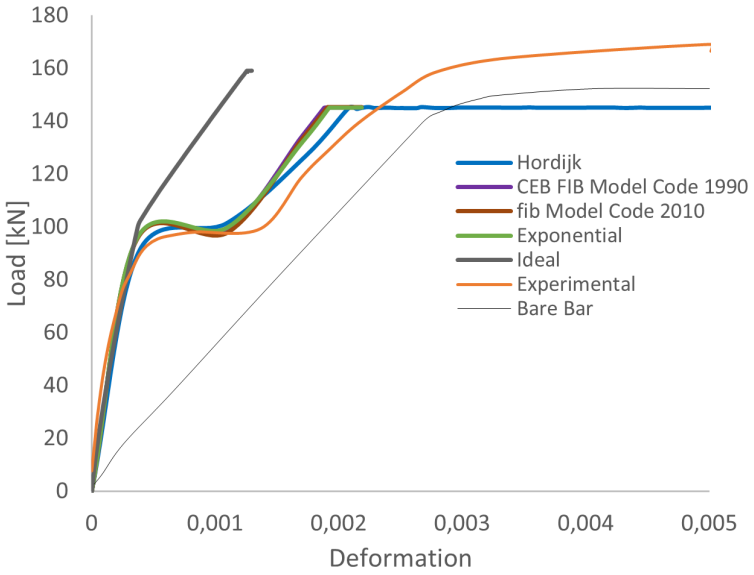

Figure 8. Study of the tensile curves of the concrete material.

With Fig. 9 it is possible to analyze separately and compare the numerical curve that presented the greatest capacity to represent the behavior of the experimental result [17] through the load-strain graph.

It is noted that the curve obtained is able to satisfactorily represent the four typical phases of tensile stiffening behavior, that is, elastic phase, crack development phase, crack stabilization phase, region where the steel supports almost entirely the tensile stresses showing that the composite still resists the increasing load and finally the yielding phase of the steel, presenting a behavior similar to that predicted in Fig. 1.

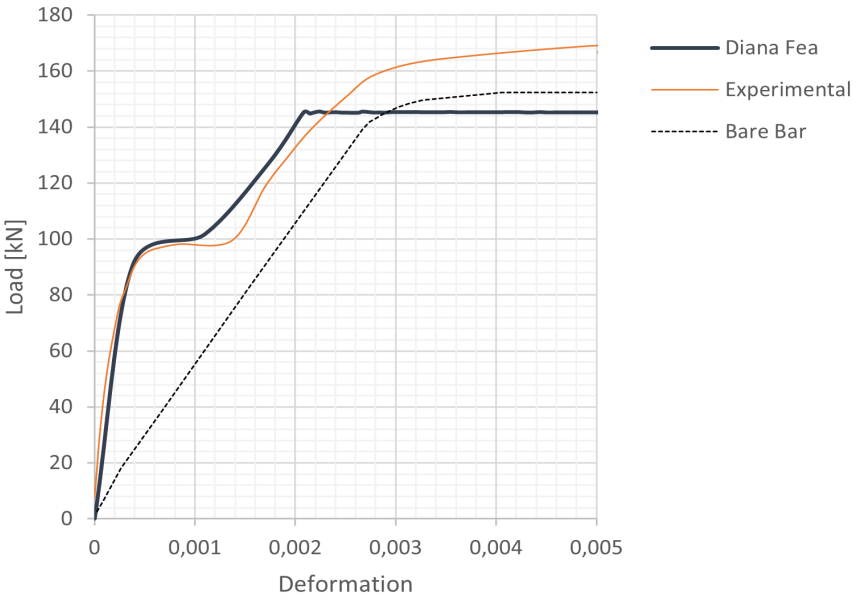

Figure 9. Load x Deformation Comparison.

After the elastic region, it is possible to observe a line with a constant force base where the cracks begin followed by an ascending stretch, where the deformations increase and the stiffness of the tie decreases.

Analyzing the numerical curve after cracking, it is possible to verify the tensile stiffening behavior in the model due to the presence of a higher load compared to the isolated bar, indicating a contribution of the concrete between the cracks (see Fig. 10).

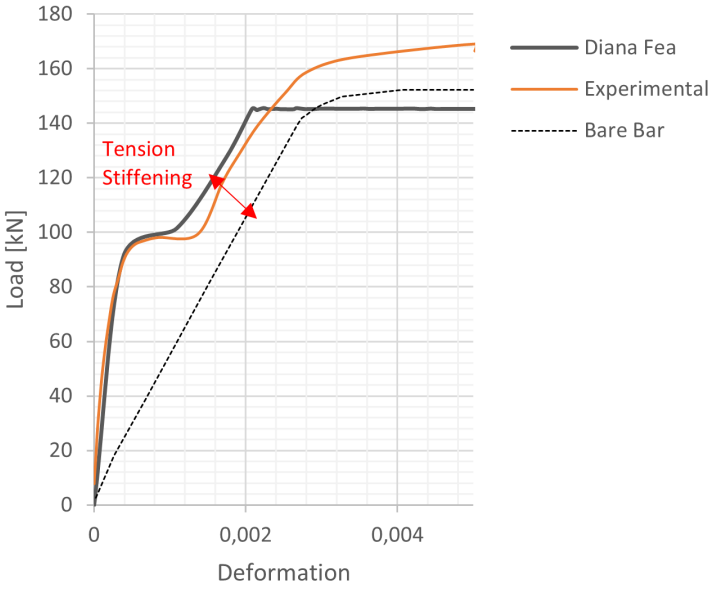

Figure 10. Observed tensile stiffening behavior.

5 Conclusion

From the analysis proposed in this study, the following observations are pointed out:

1. The computational model based on the finite element method proposed in this article proved to be able to represent the effect of tensile stiffening in reinforced concrete rods. The commercial software DIANA FEA demonstrated efficiency in generating characteristic results of deformation of the tie bar along the concrete body, being possible to analyze the distribution of the deformation of the element throughout the loading process.
2. It is possible to verify in the computational model the increase of the tension of the steel and decrease of the tension in the concrete in the appearance of the cracks.
3. Different types of tensile curves were analyzed and compared with the experimental load-strain curve and none of them was able to adequately reproduce the yielding region of the steel.
4. Although the cracking pattern from the computational model can be generated, no comparison with the experimental results is available.

Acknowledgements. The authors are partially supported by the Brazilian funding agencies CNPq, and FAPERJ. This study was financed in part by the Coordenação de Aperfeiçoamento de Pessoal de Nível Superior—Brasil (CAPES)—Finance Code 001.

References

[1] Oleg Radaykin, "Theoretical foundations of the diagram method for calculating rod elements made of reinforced concrete". *E3S Web of Conferences,* 2021.
[2] M. Baena et al., "Analysis of cracking behaviour and tension stiffening in FRP reinforced concrete tensile elements" *Composite: Part B,* 2012.
[3] Minghong Qiu, et al., "Effect of reinforcement ratio, fiber orientation, and fiber chemical treatment on the direct tension behavior of rebar-reinforced UHPC" *Construction and Building Materials"*, 2020.
[4] Said M. Allam et al., "Evaluation of tension stiffening effect on the crack width calculation of flexural RC members" *Alexandria Engineering Journal,* 2012.
[5] Miglietta, P.C et al., "Finite/discrete element model of tension stiffening in GFRP reinforced concrete" *Engineering Structures",* 2016.
[6] L.A. Oliveira Júnior et al., "Influence of steel fibers and mineral additions on cracking behavior of reinforced concrete tension members" *Revista Ibracon de Estruturas e Materiais",* 2009.
[7] Seong-Cheol Lee et al,. "Model for post-yield tension stiffening and rebar rupture in concrete members", *Engineering Structures,* 2011.
[8] H.Q. Wu and R.I. Gilbert, "Modeling short-term tension stiffening in reinforced concrete prisms using a continuum-based finite element model", *Engineering Structures,* 2011.
[9] Martins, M. P. et al,. "Modelling of tension stiffening effect in reinforced recycled concrete" *Revista Ibracon de Estruturas e Materiais",* 2020.
[10] I. Vilanova et al,. "Numerical simulation of bond-slip interface and tension stiffening in GFRP RC tensile elements" *Composite Structures,* 2016.
[11] G.A. Hegemier, et al., " On tension stiffening in reinforced concrete" *Mechanics of Materials*, 1985.
[12] D.Z. Yankelevsky et al. "One-dimensional analysis of tension stiffening in reinforced concrete with discrete cracks", Engineering Structures 30 (2008) 206–217.
[13] A. Meda et al., *"Experimental investigation on the behavior of concrete ties reinforced with GFRP bars"* Composite Structures 254, 2020.
[14] Diana Fea BV. *Diana Documentation release 10.5.* 2021.
[15] C. Santana Rangel et al., *"Tension stiffening approach for interface characterization in recycled aggregate concrete",* Cement and Concrete Composites 82, 2017, 176-189.

[16] D.M. Moreno et al., *"Tension stiffening in reinforced high performance fiber reinforced cement-based composites"*, Cement & Concrete Composites 50, 2014, 36–46.
[17] Oliveira Júnior et al., *"Tension stiffening of steel-fiber-reinforced concrete",* Acta Scientiarum. Technology, 2016.
[18] C.-C. Hung et al., *"Tension-stiffening effect in steel-reinforced UHPC composites: Constitutive model and effects of steel fibers, loading patterns, and rebar sizes"* Composites Part B 158, 2019, 269–278.
[19] Diana Fea BV. *"Tensile Test Specimen".* Tutorial Diana Fea, https://dianafea.com.
[20]G. Somma et al., "*A new cracking model for concrete ties reinforced with bars having different diameters and bond laws"* Engineering Structures 235, 2021.